

Comparison of SeaWiFS measurements of the Moon with the U.S. Geological Survey lunar model

Robert A. Barnes, Robert E. Eplee, Jr., Frederick S. Patt, Hugh H. Kieffer,
Thomas C. Stone, Gerhard Meister, James J. Butler, and Charles R. McClain

The Sea-Viewing Wide-Field-of-View Sensor (SeaWiFS) has made monthly observations of the Moon since 1997. Using 66 monthly measurements, the SeaWiFS calibration team has developed a correction for the instrument's on-orbit response changes. Concurrently, a lunar irradiance model has been developed by the U.S. Geological Survey (USGS) from extensive Earth-based observations of the Moon. The lunar irradiances measured by SeaWiFS are compared with the USGS model. The comparison shows essentially identical response histories for SeaWiFS, with differences from the model of less than 0.05% per thousand days in the long-term trends. From the SeaWiFS experience we have learned that it is important to view the entire lunar image at a constant phase angle from measurement to measurement and to understand, as best as possible, the size of each lunar image. However, a constant phase angle is not required for using the USGS model. With a long-term satellite lunar data set it is possible to determine instrument changes at a quality level approximating that from the USGS lunar model. However, early in a mission, when the dependence on factors such as phase and libration cannot be adequately determined from satellite measurements alone, the USGS model is critical to an understanding of trends in instruments that use the Moon for calibration. This is the case for SeaWiFS. © 2004 Optical Society of America

OCIS codes: 010.0010, 120.0120, 120.0280, 120.5630.

1. Introduction

The Sea-Viewing Wide Field-of-View Sensor (SeaWiFS) is a second-generation ocean color instrument. As such, its mission was designed in very large part on the lessons learned from its predecessor, the Coastal Zone Color Scanner (CZCS).^{1,2} Contractually, SeaWiFS was the procurement of an ocean color data set by the U.S. government, not an instrument of the government's design³; however, the performance specifications for the instrument included a requirement for direct lunar views to monitor instru-

ment stability.³ In addition, the performance specifications called for either an internal light source or a solar diffuser as a second monitor of instrument change. The manufacturer of SeaWiFS chose to incorporate a solar diffuser. These design decisions have had a fundamental effect on the stability-monitoring program for SeaWiFS.

SeaWiFS was launched on 1 August 1997 onboard the SeaStar spacecraft (now called Orbview-2). The first images of the Earth were taken on 4 September 1997, and the first lunar measurements were made on 14 November 1997. Since then, lunar measurements have been made on a monthly basis. The SeaWiFS calibration team does not, as yet, use the Moon as an absolute radiometric standard for calibration purposes. The Moon is used solely as a diffuse reflector whose surface remains unchanged.⁴

From the outset, the SeaWiFS calibration team did not consider itself to be expert on the surface properties of the Moon. In particular, the team was unable to account for the effects of lunar libration, in which the face of the Moon as seen from the Earth varies over time owing to a slow, periodic wobble of the Moon as it moves through its orbit. As the Moon has an inhomogeneous surface, with a pattern that can be seen from the Earth, the wobble causes a

R. A. Barnes (rbarnes@seawifs.gsfc.nasa.gov), R. E. Eplee, Jr., and F. S. Patt are with the Science Applications International Corporation, Beltsville, Maryland 20705. H. H. Kieffer (emeritus) and T. C. Stone are with the United States Geological Survey, Flagstaff, Arizona 86001. G. Meister is with the Futuretech Corporation, Greenbelt, Maryland 20770. J. J. Butler is with the Laboratory for Terrestrial Physics and C. R. McClain is with the Laboratory for Hydrospheric Processes, both at the National Aeronautics and Space Administration Goddard Space Flight Center, Greenbelt, Maryland 20771.

Received 26 December 2003; revised manuscript received 12 July 2004; accepted 27 July 2004.

0003-6935/04/315838-17\$15.00/0

© 2004 Optical Society of America

time-dependent change in the lunar irradiance. With the Moon acting as a diffuse reflector of sunlight, this change in irradiance comes from variations in the incidence and the scattering angles of the illuminating and reflected flux from its surface. For incident flux, the angles are parameterized in terms of the lunar (selenographic) latitude and longitude of the subsolar point. For scattered flux, the angles are parameterized in terms of the selenographic latitude and longitude of the subsatellite point.

With the published description of the U.S. Geological Survey (USGS) lunar irradiance model,⁵ it was recognized by the calibration team that the phase and libration factors in that model are derived empirically, that is, from observations of the Moon by the USGS telescope. As a result, the SeaWiFS calibration team has developed a set of libration corrections based on the long-term set of SeaWiFS lunar measurements. This development has been made possible, in large part, by the limitation of the SeaWiFS measurements to a small set of lunar phase angles. The phase angle is the angle between the Moon–Sun vector and the Moon–observer vector. The change in phase angle over a lunar month is the dominant factor in the cyclical changes in the brightness of the Moon and, therefore, in the USGS lunar model, which covers phase angles from 90° before full phase to 90° after.^{5,6} It is a much smaller factor in the SeaWiFS lunar measurements and thus greatly simplifies the analysis by the team.

In Section 2 we present the SeaWiFS measurements of the Moon, plus corrections to remove non-instrumental effects, including libration, from the lunar time series. In that section we also describe the time-dependent changes in the SeaWiFS bands derived from the lunar measurements. In Section 3 we give an overview of the USGS telescope and the lunar model based on its measurements, and in Section 4 we compare the SeaWiFS measurements of the Moon (after correction for the time-dependent changes in the SeaWiFS bands) with the corresponding values calculated from the USGS model.

2. SeaWiFS Lunar Measurements

A. SeaWiFS Instrument Overview

SeaWiFS is an eight-band filter radiometer. The bands have nominal center wavelengths of 412, 443, 490, 510, 555, 670, 765, and 865 nm. SeaWiFS consists of a scanner, which contains the optics, detectors, preamplifiers, and scan mechanisms, and an electronics module, which contains the signal conditioning, command, telemetry, and power supply electronics. The SeaWiFS scanner is illustrated in Fig. 1. Light from the Earth first strikes the primary mirror and then is reflected from the polarization scrambler and from the half-angle mirror before entering the aft optics. The primary mirror and the polarization scrambler are mounted upon a cylinder that rotates six times per second, and the half-angle mirror rotates at half that rate. For lunar measurements SeaWiFS views the Moon in the same manner

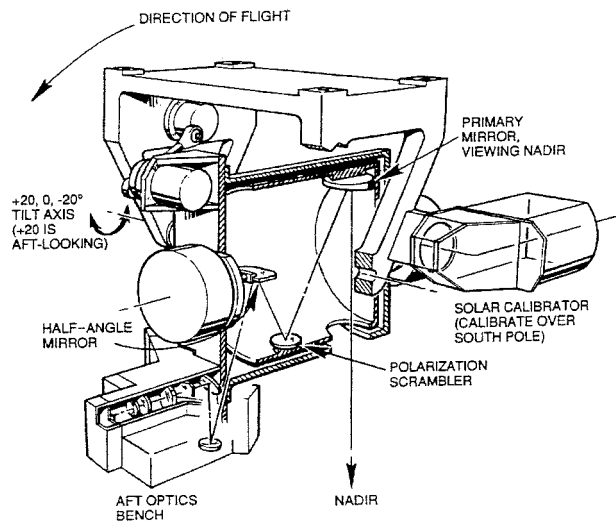


Fig. 1. Illustration of the SeaWiFS scanner.

as it views the Earth. Additional details of the design of SeaWiFS are given by Barnes *et al.*^{7,8} Results of its prelaunch characterization are given by Barnes *et al.*³

SeaWiFS operates in a polar orbit, crossing the equator from north to south at local noon. In normal operation the spacecraft is maintained in a nadir orientation, using pitch-axis momentum wheels for attitude control. For lunar measurements the rotation rate of the momentum wheels is increased, and the spacecraft is pitched in the opposite direction at a rate faster than that of normal operation. The maneuver is timed such that SeaWiFS will view the Moon as the spacecraft Earth's track passes over the sublunar point on the dark side of the Earth. At the end of the maneuver the pitch rate is returned to normal. This maneuver allows SeaWiFS to view the Moon in the same manner as it views the Earth.

Inasmuch as the Moon appears to be a stationary object during SeaWiFS measurements, the number of scan lines in a lunar measurement depends on the pitch rate of the instrument and on the apparent size of the Moon. The pitch maneuver causes SeaWiFS to oversample the Moon. There are approximately 25 scan lines of the Moon in the lunar image, whereas the Moon has a diameter that is equivalent to approximately 7 SeaWiFS samples. Additional details of the lunar maneuver and the lunar sampling procedures are given by Barnes *et al.*^{9,10} The uncertainty in the number of scan lines in a SeaWiFS lunar image is a principal source of error in the measurements.

B. Geometry, Phase, and Oversampling Factors

At the time of the first SeaWiFS lunar measurement, no lunar model was available to the SeaWiFS calibration team. As a result, the team developed a limited set of normalizing factors for the measurements, such as the Sun–Moon distance and the

Moon–instrument distances.^{9,10} As the team uses the Moon to determine long-term instrument changes only, the reference values for the normalizations are set to unity at the start of the mission.

SeaWiFS makes measurements of the input radiance ($\text{mW cm}^{-2} \mu\text{m}^{-1} \text{sr}^{-1}$) within each $1.6 \text{ mrad} \times 1.6 \text{ mrad}$ pixel. For lunar measurements, 22×33 pixel images are assembled.^{9,10} These images include both the Moon and a surrounding region of pixels of black space. For each SeaWiFS band the radiances from the pixels in the image are summed to give integrated lunar radiances:

$$S_n = \sum_{i=1}^{N_p} L_{i,n}, \quad (1)$$

where S_n is the summed radiance for SeaWiFS band n , N_p is the number of samples (726) in the SeaWiFS lunar image, and $L_{i,n}$ is the radiance for sample i , band n ($\text{mW cm}^{-2} \mu\text{m}^{-1} \text{sr}^{-1}$).

Normalizing factors are applied to these summed radiances to remove, as best as possible, noninstrumental effects in the measurements. The first normalizing factors make corrections to standard Earth–Sun and Moon–instrument distances:

$$S_{\text{An}} = S_n \left(\frac{D_{\text{SM}}}{1 \text{ AU}} \right)^2 \left(\frac{D_{\text{MV}}}{384,400 \text{ km}} \right)^2, \quad (2)$$

where S_n is the summed lunar radiance for band n , D_{SM} is the Sun–Moon distance [in astronomical units (AU)], D_{MV} is the Moon–Viewer distance (km), 1 AU is the mean radius of the Earth’s orbit about the Sun, 384,400 km is the mean radius of the Moon’s orbit about the Earth, and S_{An} is the normalized radiance. The second normalizing factor corrects the radiances to a standard phase angle of 7° :

$$S_{\text{Bn}} = S_{\text{An}} \left(\sum_{i=0}^2 v_i g^i \right) (1 + \varepsilon_n [g - 7]), \quad (3)$$

where S_{Bn} includes this normalization. The summation term in Eq. (3) is a second-order polynomial in lunar phase^{9,10} based on the lunar reflectance model of Helfenstein and Veverka,¹¹ which is itself based on the measurements of Lane and Irvine.¹² Helfenstein and Veverka¹¹ used the average of those measurements, at wavelengths from 360 to 1600 nm, to create a single, best-fit lunar reflectance curve at an undefined wavelength, presumably near 500 nm. Coefficients v_i have been set up to give a value of unity at 7° lunar phase, and the units of these coefficients are such that the normalization is dimensionless. Such is also the case for the other normalizations in this section. The second term in Eq. (3) is an empirically derived, wavelength-dependent correction based on the SeaWiFS lunar measurements.^{13,14} Coefficient ε_n (dimensionless) in the second term is small, with differences among the bands of approximately 1%.

Because changes in phase angle cause dramatic changes in the brightness of the Moon, the decision was made to keep the phase angles of the measure-

ments at approximately 7° to minimize the effect. The phase of the Moon changes by $\sim 0.75^\circ$ during a SeaWiFS orbit, so it was anticipated that the variation in the measurements would be less than 0.5° from 7° . However, early in the mission, conflicts between the timing of the lunar measurements and the transmission of satellite data to the ground required occasional measurements at phase angles more than 2° from the standard angle. The wavelength-dependent correction adjusts for the effects of these phase angle differences.^{13,14} In addition, the flight operation procedures for SeaWiFS have been modified to minimize the differences of the phase angles from 7° .

The original correction used by the SeaWiFS calibration team included a term for the illuminated area of the Moon, which is also a function of the lunar phase angle.^{9,10} However, it is now known that the illuminated area is part of the values of Helfenstein and Veverka.¹¹ On average, the effect of the erroneous incorporation of the illumination area is small, $\sim 0.1\%$. It is no longer used in the processing of the SeaWiFS lunar data set.

The rotation rate of the spacecraft during the measurement causes an elongated lunar image (see Barnes *et al.*^{9,10}). In other words, the Moon is oversampled during the measurement. The normalization for this noninstrumental effect is made by use of Eq. (4):

$$S_{\text{Cn}} = S_{\text{Bn}} \left(\frac{3474.8 \text{ km}/D_{\text{MV}}}{Y_M} \right), \quad (4)$$

where S_{Cn} is the summed radiance after normalization and Y_M is the size of the Moon in the along-track direction. The oversampling correction in Eq. (4) represents a significant change from the previous correction by Barnes *et al.*¹⁰ In that normalization, the extent of the Moon in the along-track direction, which is the direction of oversampling, was determined as the point in the image where the instrument response was 1% of the maximum. Here the normalization is calculated as the ratio of the along-track angular diameter of the Moon as viewed by the SeaWiFS instrument to the Moon’s actual angular diameter. The actual angular diameter of the Moon is the physical lunar diameter (3474.8 km) divided by the Moon–instrument distance (D_{MV}) in kilometers.

The size of the Moon in the along-track direction (Y_M) comes from the images themselves, as there is no means of accurately determining the spacecraft’s rotation rate during the lunar maneuver. The objective is to determine the locations of the pixels at the top and the bottom of the lunar image that are 50% illuminated by the lunar disk. The size is determined by use of a modified version of an edge detection routine in the IDL programming language. This routine determines the first and second derivatives, as functions of pixel number, in along-track sections of the lunar images. An example of such an along-track profile is shown in Fig. 2. The profile comes from Fig. 2 of Barnes *et al.*¹⁰ and is shown to

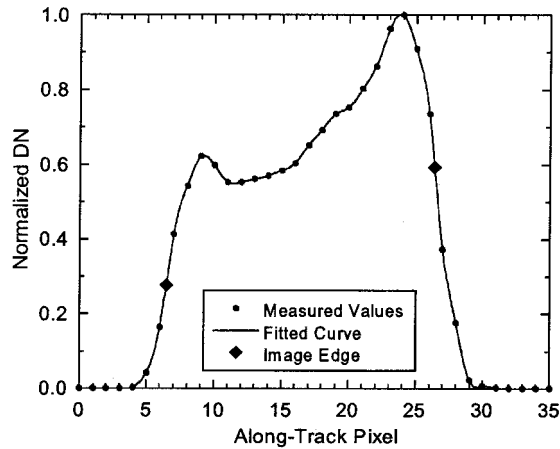


Fig. 2. Along-track section of the Moon measured by SeaWiFS. This comes from Fig. 2 of Barnes *et al.*¹⁰ and has been normalized to the range from zero to unity. The diamonds give the calculated edges for the cross section. DN, digital numbers.

illustrate the basic procedure. The small circles give the SeaWiFS-measured values, and the line is a fitted curve. The diamonds give the locations of the maximum and minimum in the first derivative. However, because of the shape of the profile, other maxima and minima also occur. To account for possible ambiguities, the procedure uses the zero-crossing point for the second derivative that occurs closest to the first pixel that is partially illuminated by the Moon coming from the off-the-Moon direction. This zero-crossing (or inflection) point provides the location of the maximum rate of change in the SeaWiFS-measured values. This procedure is repeated for each set of along-track measurements by the instrument. The longest distance, from image edge to image edge, gives the size of the Moon. With this procedure, the along-track size of the Moon is approximately 20 pixels for the SeaWiFS measurements. It is estimated that the uncertainty in this size calculation is approximately 0.5 pixel, or $\sim 2.5\%$ of the calculated value. The major contribution to this uncertainty comes from the calculation of the edges of the lunar image.

A second contribution to the oversampling uncertainty comes from the misalignment of the along-track direction of the spacecraft and the long axis of the illumination of the Moon by the Sun.¹⁵ When the Moon is measured diagonally across its illuminated surface, the along-track size of the illuminated Moon is always smaller than the actual diameter of the Moon. This effect is also dependent on the phase angle for the lunar measurement. For measurements near 7° phase, this effect is small, ranging from zero to 0.3%. For measurements with nearly identical phase angles, the effect adds to the scatter in the time series. However, this additional scatter is small compared with the scatter from the calculation of the edges of the lunar image, and no misalignment correction is applied to the measurement here.

For lunar measurements it is important to ensure,

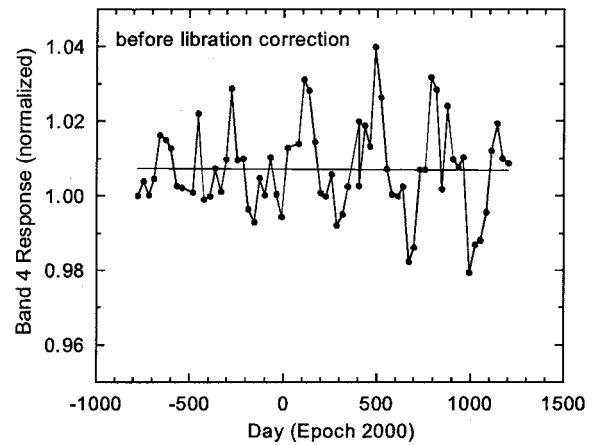


Fig. 3. Response of band 4 before correction for libration. The responses are normalized to the initial value. The straight line gives a linear fit to the responses. Epoch 2000 has a reference of unity for the first day of the year 2000.

as best as possible, that the measurements from the instrument uniformly cover the Moon's surface—with no gaps between pixels and with no overlaps. Laboratory measurements have shown the SeaWiFS pixels to be approximately square,³ with cross-sectional areas equivalent to squares with side lengths of 1.60 ± 0.03 mrad. The average side length of 1.60 mrad is used to convert the along-track size of the Moon from pixels to radians in the oversampling correction.

C. Libration Factor

For the SeaWiFS calibration team the libration normalization terms are empirically determined from the set of SeaWiFS lunar observations. They come from an analysis of the values of S_{CN} , that is, from the lunar time series after the removal of distance, phase angle, and oversampling effects. The normalizations use the values from band 3 (490 nm), band 4 (510 nm), and band 5 (555 nm). Within the full set of SeaWiFS bands the long-term changes in these bands are small. The response of band 4, before libration correction, is shown in Fig. 3. It is representative of the responses of bands 3 and 5, also. Figure 3 shows the values of S_{CN} from Eq. (4) normalized to unity for the first lunar measurement. The figure also shows a fit to the data points by linear regression. The slope of the fitted line is not crucial to this normalization. However, its form as a straight line is important. At the conclusion of the normalization for libration, the resultant trends in bands 3–5 are straight lines. The linear form of these calculated trends may be influenced by the manner in which the libration normalization is applied. However, if these trends are small, the deviations in the actual instrument trends from the calculated straight lines should also be small.

The normalization uses the ratios of the measured points for bands 3–5 from each of their linear regressions (Fig. 3). It is assumed that the libration effects

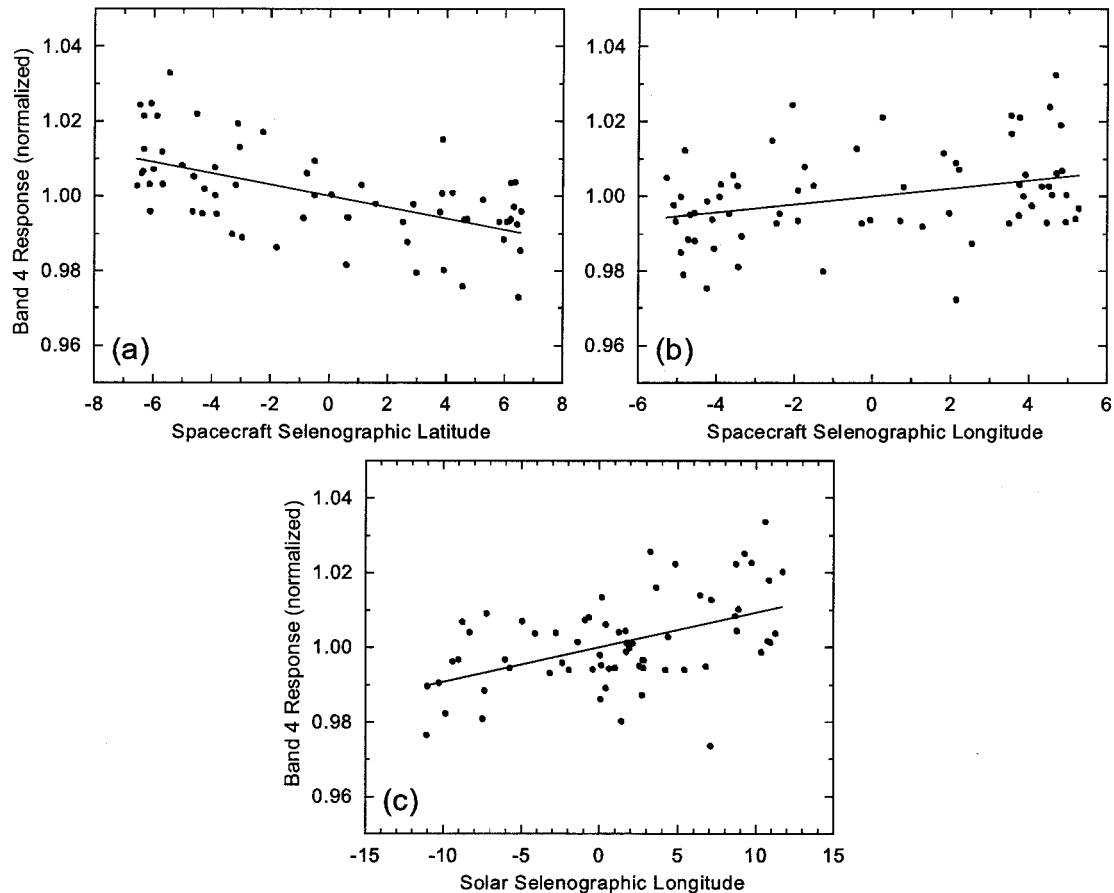


Fig. 4. Dependencies of the SeaWiFS measurements on the lunar libration variables. The data points give the residuals about the line in Fig. 3 for each variable. The lines give the linear fits for these residuals.

are the same for all wavelengths, so bands 3–5 are representative of the other SeaWiFS bands. These ratios can be represented as dependent variables of any of the libration variables. For the SeaWiFS libration normalization, the independent variables of solar selenographic longitude, spacecraft selenographic latitude, and spacecraft selenographic longitude are used. And, for this normalization, linear dependencies are calculated.

The dependencies for these variables are shown in Fig. 4. This figure gives the residuals about the line in Fig. 3 plotted versus the libration variables plus the linear fits for the residuals. The slopes of these lines provide the effects for the libration variables. The calculated effects for the three libration variables, as functions of time, are shown in Figs. 5(a)–5(c). Figure 5(d) shows the product of the individual effects. The pattern in Fig. 5(d) reflects the basic pattern in Fig. 3, and it is this pattern that the libration correction removes. The spacecraft's latitude and longitude are periodic functions with different frequencies, and the effect of the difference is evident in the total effect. The solar longitude effect in Fig. 5(c) is not a smooth function with time, as SeaWiFS makes lunar measurements both before and after full phase in the lunar cycle. In addition, there is a small but noticeable phase angle dependence in the

data set before the libration correction, with the values for the waxing Moon slightly different from those of the waning Moon. However, this dependence is removed by the libration normalization.

The libration normalization takes the form

$$S_{Dn} = S_{Cn}[(1 + w_1\Phi)(1 + w_2\theta)(1 + w_3\phi)]^{-1}, \quad (5)$$

where S_{Dn} is the summed radiance after normalization and w_1 , w_2 , and w_3 are the coefficients for the solar selenographic longitude (Φ), the spacecraft selenographic latitude (θ), and the spacecraft selenographic longitude (ϕ), respectively. The latitude and longitudes have units of degrees, and the coefficients have units of inverse degrees. The coefficients are calculated by use of linear regressions, and the normalizations are unity at 0° selenographic latitude and longitude. The terms in Eq. (5) give the libration effects, and the correction is calculated as the inverse of the overall effect. For each libration coefficient, the values of the coefficients for the three individual bands disagree from the average by less than 5%.

The SeaWiFS libration corrections are a simplified version of the terms in the USGS lunar model described in Subsection 3.B below. There are no combined terms of the form $\Phi\phi$ or $\Phi\theta$, as the Moon is near

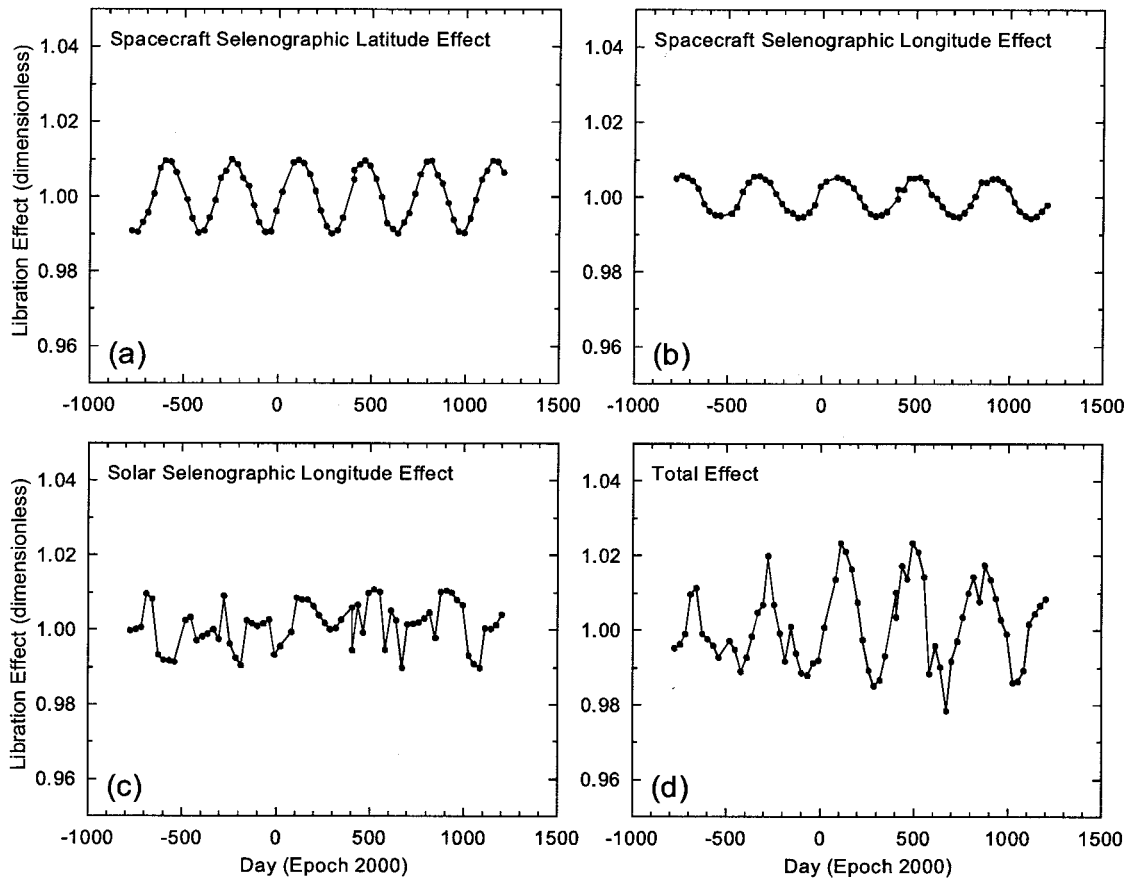


Fig. 5. Calculated libration effects for SeaWiFS band 4. The normalization factors are the inverses of the effects.

full illumination and the solar selenographic longitudes for the SeaWiFS measurements are small. These combined terms are significant at large solar longitude angles when the Moon is partially illuminated and the uneven distribution of bright and dark features on the lunar surface become a factor in the measurements. There is also no term in Eq. (5) to account for the opposition effect,¹⁶ because that effect occurs primarily at phase angles less than 4° , smaller than those for the SeaWiFS measurements. In addition, there is no term in the normalization procedure to account for residual correlations among the libration variables. However, the libration correction was calculated in a two-step process, with a second iteration of the procedure to remove residual libration dependencies in the first step. Finally, there is no solar selenographic latitude term in Eq. (5) to correspond to the spacecraft's selenographic latitude. The effects of spacecraft and solar selenographic latitudes are correlated, and the spacecraft's latitude provides a satisfactory correction by itself.

Figure 6 shows the response of SeaWiFS band 4 before and after libration correction. Figure 6(a) is the same as Fig. 3. It is shown for comparison with Fig. 6(b), which gives the response after correction. Figure 6(b) shows a scatter about the fitted line of $\sim 0.75\%$, 1σ . However, that scatter does not show periodicities with the frequencies of those in Fig. 6(a).

If there is a residual libration component in Fig. 6(b), it is lost in the measurement-to-measurement scatter, which is thought to come from the oversampling correction in Eq. (4). It has a magnitude that is consistent with the uncertainty estimated for the correction.

D. Oversampling Error

The measurement-to-measurement scatter in the oversampling correction provides a major limitation in the determination of long-term instrument changes that use the Moon. For each measurement the oversampling calculation adds an uncertainty to the SeaWiFS lunar irradiance. This is a systematic error that is present to the same degree in all the bands. For the lunar time series the error appears as a scatter in the trends, as it changes from measurement to measurement. The scatter affects the calculated trends as new measurements are added to the data set. Figure 7 shows this effect for SeaWiFS band 4. The figure shows the time series of the calculated linear trends for the values from Fig. 6(b). The linear trend calculated for measurements 1–6 is $+1.1\%$ per thousand days. With the addition of measurement 7, the trend becomes $+1.9\%$ per thousand days. The addition of measurements 8–10 drives the calculated slope negative. As new measurements con-

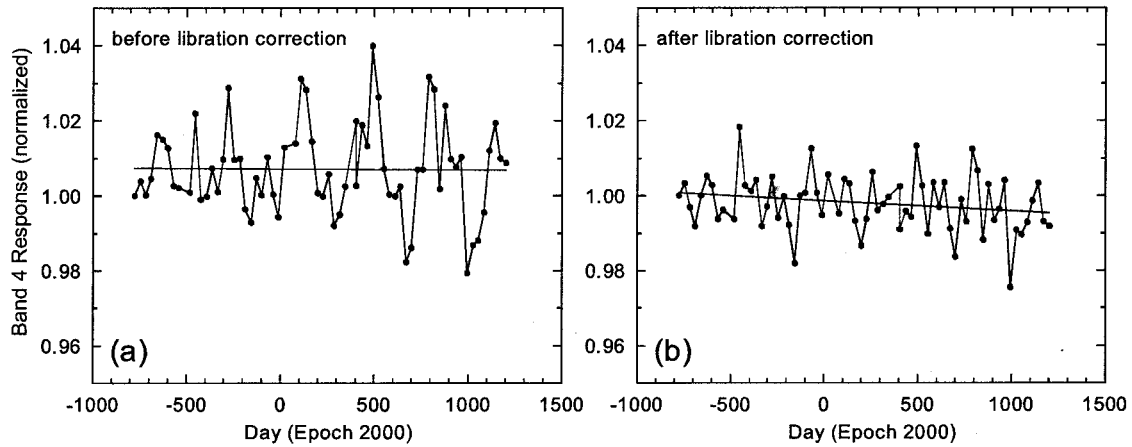


Fig. 6. Response of band 4 before and after correction for libration. The responses are normalized to the initial values. The lines give linear fits to the responses.

tinue to accumulate, this oscillation in the calculated slopes dampens out. For SeaWiFS an extended set of measurements is required for overcoming the effects of the measurement-to-measurement scatter.

The oversampling scatter is inherent in the current analysis procedure for the SeaWiFS lunar measurements. Its effects are also part of the comparison with the USGS lunar model in Section 4 below. However, with a set of 66 lunar measurements covering approximately 5.5 years, its effects are greatly reduced. For the last seven measurements in the data set (Fig. 7) the calculated slopes for band 4 have varied by less than 0.1% per thousand days. Finally, the residual scatter from the oversampling error is virtually the same for all the SeaWiFS bands.

To correct for this error it is possible to calculate the fractional difference of each data point from the fitted line in Fig. 6(b), and this process can be repeated for

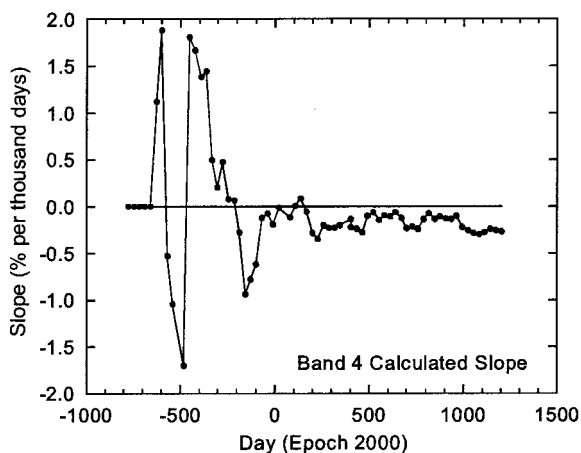


Fig. 7. Calculated slopes for the response of SeaWiFS band 4. The slopes are calculated by use of linear fits. The unit for the slopes is percent change per thousand days. The slope for measurements 1–6 is +1.1%. The slope for measurements 1–7 is +1.9%. The slope for measurements 1–66 is -0.27% . No slope was calculated for measurements 1–5. The change in slope, as new measurements are added, dampens over time.

SeaWiFS bands 3 and 5. When the fractional differences for the three bands are averaged, the result is an oversampling scatter correction that can be applied to all the SeaWiFS bands. The correction is the inverse of the average fractional difference. Figure 8(a) shows the response of band 4 with the removal of the oversampling scatter. Figure 8(a) shows the response before the removal. It is a duplicate of Fig. 6(b), except for an expanded vertical scale.

The removal of the oversampling scatter does not effect the slope for band 4. The slope is the same for both parts of Fig. 8. Nor does the removal affect the slopes for bands 3 or 5. Ultimately, the oversampling correction does not effect the slopes for the other SeaWiFS bands—bands that change in a nonlinear fashion with time. However, the oversampling correction does reveal the shape of the nonlinearities (see Fig. 9), and, with the shape revealed, it is possible to develop the form for the fitted curves. Those fitted curves, described in Subsection 2.E below, apply equally well to the measured results with, and without, the removal of the oversampling error. The oversampling correction, however, is a step in their development.

E. Instrument Changes on Orbit

Figure 9 shows the responses of all eight SeaWiFS bands, each with the same correction for oversampling scatter. For bands 1–6 the changes are less than 2%. For band 7 the change is less than 5%, and for band 8 the change is approximately 13%.

For these calculations to work, it is necessary to know that the instrument's response is changing smoothly over time, without discontinuities. Discontinuities of this sort were present in the measurements of CZCS,¹⁷ the predecessor to SeaWiFS. As a result, a solar diffuser was incorporated into the SeaWiFS instrument. Daily measurements of the solar irradiance reflected from the diffuser¹⁸ have shown no discontinuities in the response of SeaWiFS.

For each band in Fig. 9 there is a fitted curve. For

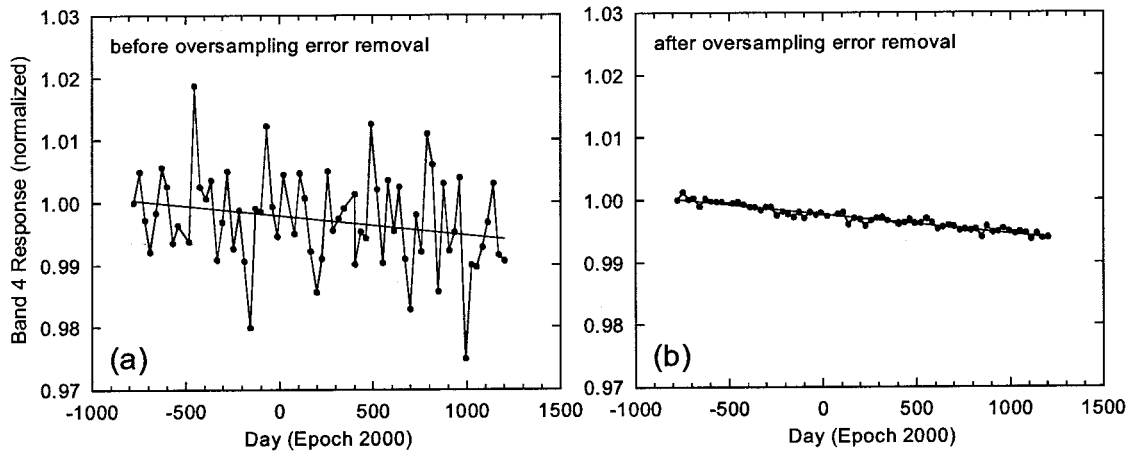


Fig. 8. Response of band 4 before and after removal of the oversampling error. The responses are normalized to the initial values. The lines give linear fits to the responses. The slopes for the two linear fits are identical. (a) Same as Fig. 6(b), except for an expanded vertical scale here.

bands 3–5 the curves are straight lines. For bands 1, 2, and 6 the curves are single exponentials with time constants of 2000 days. For bands 7 and 8 the curves are combinations of two exponentials, one with a shorter time constant (200 days) and one with

a longer time constant (2000 days). The general equation for the eight bands,

$$y = z_0 + z_1 t + z_2 \exp(-z_3 t) + z_4 \exp(-z_5 t), \quad (6)$$

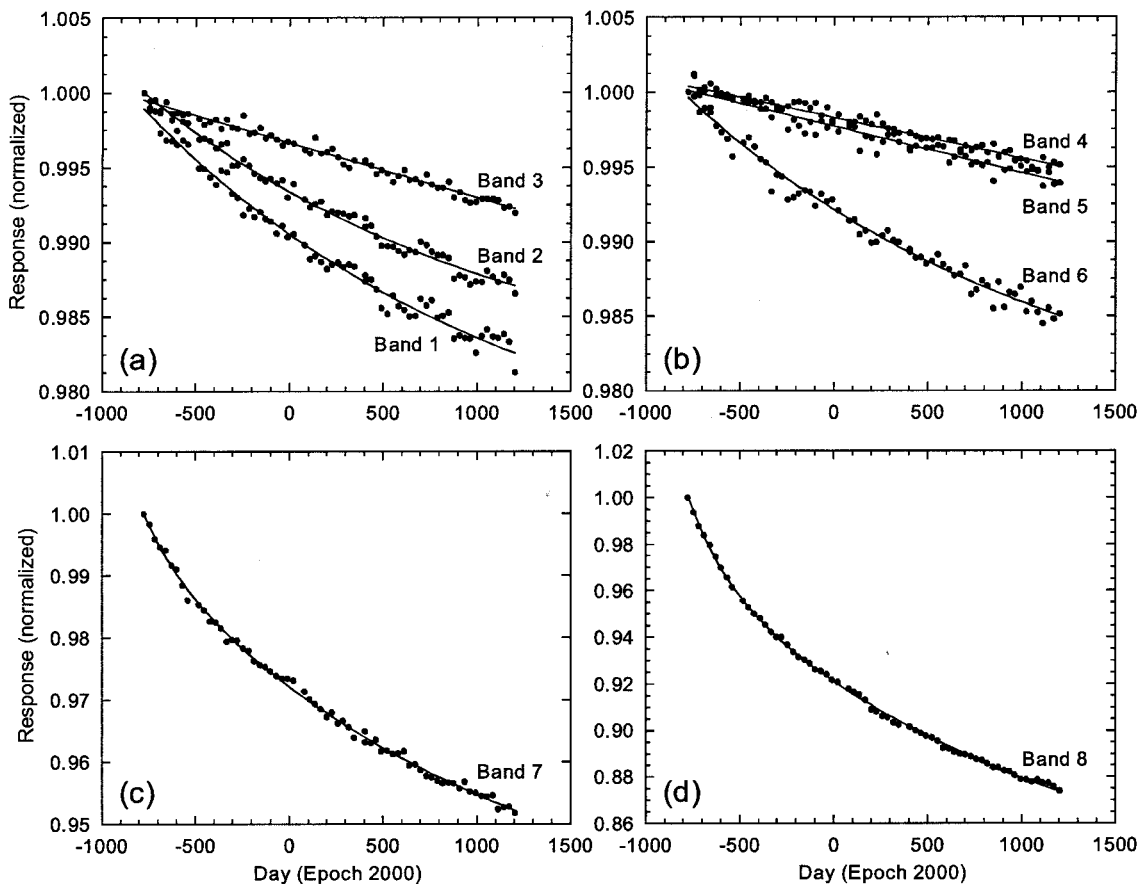


Fig. 9. Responses of the SeaWiFS bands. The responses are normalized to the initial values. The lines are fitted curves. For bands 3–5 the fitted curves are linear. For bands 1, 2, and 6–8 the fitted curves are exponentials.

Table 1. Coefficients for the Fitted Curves in Fig. 9^a

Band	Wavelength (nm)	z_0	z_1	z_2	z_3	z_4	z_5
1	413.0	0.9729	0	0.0260	0.0005	0	0
2	444.1	0.9794	0	0.0206	0.0005	0	0
3	490.1	0.9995	-3.677×10^{-6}	0	0	0	0
4	510.3	1.0004	-2.727×10^{-6}	0	0	0	0
5	554.2	1.0001	-3.098×10^{-6}	0	0	0	0
6	668.8	0.9764	0	0.0232	0.0005	0	0
7	763.8	0.9282	0	0.0646	0.0005	0.0072	0.005
8	866.4	0.8167	0	0.1529	0.0005	0.0313	0.005

^aCoefficients z_0 , z_2 , and z_4 are dimensionless. Coefficients z_1 , z_3 , and z_5 have units of inverse days. The wavelengths come from Table 4 below.

includes terms for each type of curve. In Eq. (6), y is the calculated response (dimensionless), t is the time after the first measurement in the data set (in units of days), z_0 , z_2 , and z_4 are coefficients for the fitted curve (dimensionless) and z_1 , z_3 , and z_5 are coefficients in units of inverse days. The coefficients for Eq. (6) are listed in Table 1. For the data points in Fig. 9 the values are normalized to unity for the first measurement. However, the fitted curves are not forced to unity for the time of the first lunar measurement ($t = 0$, which is day -777 in Epoch 2000), as can be seen from Figs. 9(a) and 9(b).

For band 8 the responses agree with the fitted curve at the 0.1% level (see Table 2). For the other bands the agreement is better. This result is an indication that the oversampling noise is common to all the bands. In addition, the agreement between the responses and the fitted curves in Fig. 9 gives an indication of the level at which instrument trends can be determined by satellite instruments that use long-term lunar measurements.

The first SeaWiFS lunar measurement was made 105 days after the start of the SeaWiFS mission. If the instrument changes after the first lunar measurement are representative of the changes before, then it is possible to extrapolate the fitted curves in Fig. 9 back to the start of the mission to estimate the changes in the instrument before the first lunar measurement. Those changes are listed in Table 3. The extrapolations go back to two dates, to the launch of SeaWiFS and to the date on which SeaWiFS made

its first image of the Earth. The launch occurred 105 days before the first lunar measurement, and the first SeaWiFS Earth image was obtained 71 days before. During the 34 days between these two events SeaWiFS was raised to its operating orbit and was allowed to outgas. At the date of the first Earth image SeaWiFS began its normal on-orbit operations. The instrument changes and the processes for the changes during the 34-day interim period are unknown to us. Only for bands 7 and 8 are the differences between the two events significant.

For absolute comparisons with the USGS lunar model we assume that the extrapolation to the launch date, as done for the SeaWiFS transfer-to-orbit experiment¹⁹ and for the reflectance-based calibration of SeaWiFS,¹⁸ gives the best estimate of the change in the instrument before the first lunar measurement.

3. USGS Lunar Measurements

A. USGS Telescope System Overview

A program to characterize the brightness of the Moon for the on-orbit calibration of Earth remote-sensing imaging instruments has been established by the USGS.^{20,21} The basis for this program is the Robotic Lunar Observatory (ROLO), an automated observatory dedicated to the radiometry of the Moon. ROLO has been observing the Moon in the visible and the near infrared (VNIR) at wavelengths from 347 to

Table 2. Scatter in the SeaWiFS Values about Their Fitted Curves in Fig. 9^a

SeaWiFS Band	Wavelength (nm)	Standard Deviation (%)
1	413.0	0.06
2	444.1	0.04
3	490.1	0.03
4	510.3	0.03
5	554.2	0.05
6	668.8	0.06
7	763.8	0.06
8	866.4	0.09

^aThe standard deviations of the values about the curves give a measure of the scatter in the data.

Table 3. Instrument Changes before the First Lunar Measurement^a

Band	Wavelength (nm)	Change from Launch (%)	Change from First Image (%)
1	413.0	-0.14	-0.09
2	444.1	-0.11	-0.07
3	490.1	-0.04	-0.03
4	510.3	-0.03	-0.02
5	554.2	-0.03	-0.02
6	668.8	-0.13	-0.08
7	763.8	-0.85	-0.54
8	866.4	-2.98	-1.88

^aThese changes are extrapolations based on the fitted curves in Fig. 9. The launch of SeaWiFS occurred 105 days before the first lunar measurement. The first SeaWiFS image taken when the instrument was turned on occurred 71 days before the first lunar measurement.

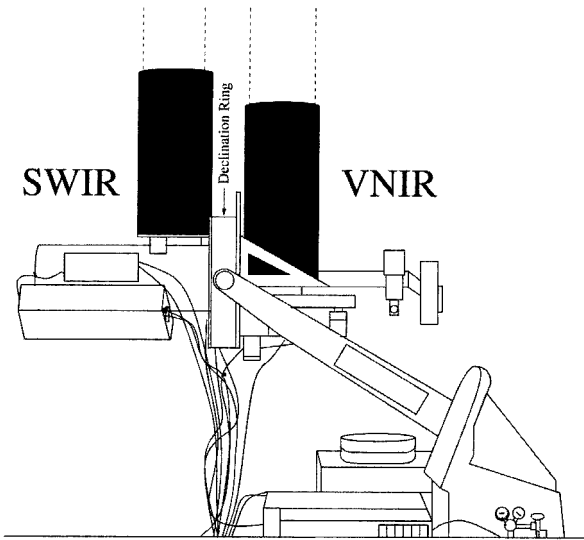


Fig. 10. Schematic of the ROLO telescope assembly. The single fork mount holds two telescopes pointed at zenith. The VNIR camera and telescope are mounted to the right of the declination ring.

945 nm since 1995 and in the short-wave infrared (SWIR) at wavelengths from 945 to 2390 nm since 1997.

The observatory is located in Flagstaff, Arizona, at the USGS Flagstaff Field Center in a specially designed dome that houses two telescopes, as shown in Fig. 10. The optical path through the VNIR telescope and camera is shown in Fig. 11. The camera uses an array chip with 512 by 512 usable square pixels.²¹ A filter enclosure mounted at the entrance to the camera head holds two identical wheels with 18 filter holes in each. The first hole position is empty in both wheels, permitting the use of the filters in the other wheel. Twenty-three filters provide measurements at wavelengths from 347 to 945 nm. The center wavelengths and bandwidths for these filters are listed in Table 4. This table also includes corresponding information for the eight SeaWiFS bands. Additional details of the VNIR and the SWIR telescope-camera systems are given by Anderson *et al.*²¹

The goal of the ROLO project is to produce a radiometrically calibrated photometric model of the Moon for all libration angles visible from Flagstaff for phase angles from 2° to 90°. However, ROLO observes standard stars as well as the Moon. During the night the Moon is observed at half-hour intervals when it is within 60° of the zenith. Between these measurements and during the remainder of the night, the telescope views the standard stars. The measurement routines observe as many stars as possible to maximize the number of calibration measurements for the telescopes. It is the stability of the ensemble of standard stars, not individual stars themselves, that is used as the photometric reference for determining long-term instrument changes.

Also during each night, a subset of the photometric

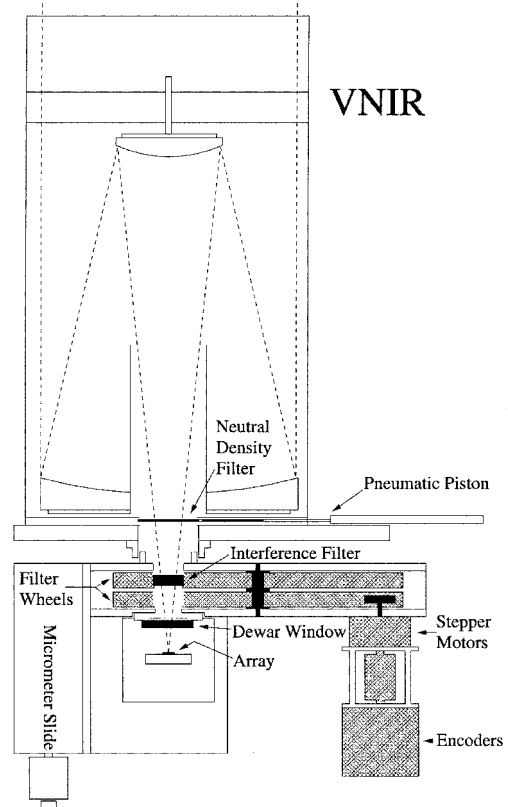


Fig. 11. Schematic of the VNIR telescope and camera optics. The dashed lines show the optical path through the instrument.

standard stars is used to determine the atmospheric extinction.⁶ Each star in this subset is measured many times over the largest number of zenith angles to maximize the range of air masses in the atmospheric correction. From these measurements the atmospheric extinction algorithm finds a least-squares solution for the abundances of absorbing gases, and their time dependence during the night. The fitting coefficients derived from this algorithm are used to provide the extinction corrections for the lunar and stellar measurements.⁶

The absolute radiance scale for the ROLO telescopes is based on measurements of the star Vega (α Lyr), which are compared with values published in the astronomical literature.⁶ Vega is one of the ROLO standard stars, visible in the night sky from April to September. From values in the literature, an exoatmospheric spectral irradiance model for Vega was developed and combined with the spectral responses for the ROLO telescope bands to give effective photon fluxes for Vega in each band. The ratios of the fluxes to the instrument response rates give the absolute radiance scales for the ROLO bands.²²

For satellite calibration purposes, the lunar surface does not change over a period of 10^8 years.⁴ However, there are cyclical changes in the radiance of the Moon, particularly over the period of a lunar month. It is the USGS model⁵ that removes these cyclical

Table 4. Center Wavelengths and Bandwidths for the ROLO VNIR Filters^a

ROLO Filter Number	Center Wavelength (nm)	Bandwidth (nm)	SeaWiFS Band Number	Center Wavelength (nm)	Bandwidth (nm)
1	347.3	32.5			
2	352.5	31.6			
3	405.0	16.2			
4	412.7	12.5	1	413.0	21.4
5	415.1	17.8			
6	441.8	9.6	2	444.1	21.0
7	466.5	20.0			
8	475.7	18.4			
9	488.1	7.9	3	490.1	22.0
			4	510.3	23.4
10	545.0	18.8			
11	550.3	8.7			
12	554.9	18.1	5	554.2	19.3
13	666.7	8.3	6	668.8	20.0
14	694.8	16.8			
15	705.5	16.7			
16	747.1	8.7			
17	765.5	16.8	7	763.8	40.9
18	776.5	16.9			
19	867.7	13.9	8	866.4	41.6
20	875.3	18.4			
21	885.2	16.0			
22	934.6	17.6			
23	944.7	18.8			

^aThese values have no corrections for the detector response or for the spectral shape of the observed radiation.²¹ The corresponding wavelengths for the SeaWiFS bands are also listed. They come from system level instrument measurements and include the response of the detectors.⁷ However, they have no corrections for the spectral shape of the observed radiation.

patterns from the lunar measurements by the ROLO telescope.

B. USGS Lunar Model

Inasmuch as the Moon overfills each sample (pixel) measured by the ROLO telescope, the measurements are made as radiance ($\mu\text{W m}^{-2} \text{nm}^{-1} \text{sr}^{-1}$). The individual samples are summed and multiplied by the solid angle for each sample to give a lunar irradiance

$$I_k' = \Omega_p \sum_{i=1}^{N_p} L_{i,k}, \tag{7}$$

where I_k' is the lunar irradiance for ROLO band k ($\mu\text{W m}^{-2} \text{nm}^{-1}$), Ω_p is the solid angle for sample i (sr^{-1}), N_p is the number of samples in the ROLO lunar image, and $L_{i,k}$ is the radiance for sample i , band k ($\mu\text{W m}^{-2} \text{nm}^{-1} \text{sr}^{-1}$). For the ROLO measurements, each lunar image includes an edge of pixels of black space. For each band the measured irradiance is reduced to the corresponding irradiance at standard Sun–Moon and Moon–Viewer distances I_k :

$$I_k = I_k' \left(\frac{D_{\text{SM}}}{1 \text{ AU}} \right)^2 \left(\frac{D_{\text{MV}}}{384,400 \text{ km}} \right)^2, \tag{8}$$

where D_{SM} is the Sun–Moon distance (AU), D_{MV} is the Moon–Viewer distance (km), and 384,400 km is the mean radius of the Moon’s orbit about the Earth.

Although the observations by the ROLO telescope

are made as radiances, the lunar model is developed in the dimensionless units of reflectance. For each ROLO band the conversion from irradiance to effective disk reflectance is

$$I_k = \frac{A_k \Omega_M E_k}{\pi}, \tag{9a}$$

where A_k is the effective disk reflectance (dimensionless), Ω_M is the solid angle of the Moon at 384,400 km ($6.4236 \times 10^{-5} \text{sr}$), and E_k is the solar irradiance at 1 AU, with the same units as I_k ($\mu\text{W m}^{-2} \text{nm}^{-1}$). Equation (9a) can be rearranged to give

$$A_k = \pi \frac{I_k / \Omega_M}{E_k}, \tag{9b}$$

where I_k / Ω_M in the numerator gives the average radiance over the entire area of the Moon ($\mu\text{W m}^{-2} \text{nm}^{-1} \text{sr}^{-1}$) for the ROLO telescope measurement. When the numerator is divided by the solar irradiance, the ratio of radiance to irradiance in Eq. (9b) is called the bidirectional reflectance distribution function (BRDF), with units of inverse steradians. The factor of π in Eqs. (9a) and (9b) converts the BRDF to the bidirectional reflectance factor (BRF).

The BRF is defined as the ratio of the radiant flux from a sample surface to that of an ideal surface irradiated in the same way.^{23,24} For an ideal diffuse surface^{23,24} the BRDF has a value of $1/\pi \text{sr}$, and the BRF, by definition, is unity (dimensionless). Thus,

for an ideal diffuse surface and for other surfaces as well, the conversion constant between BRDF and BRF has a value of π sr. In reflectance terms the value of A_k in Eq. (9b) gives the effective BRF for the disk of the Moon. Here A_k is called the equivalent disk reflectance of the Moon.

The USGS lunar model⁵ fits the results of the ROLO observations into an empirical analytic form based on primary geometric variables:

$$\ln A_k = \sum_{i=0}^3 a_{ik} g^i + \sum_{j=1}^3 b_{jk} \Phi^{2j-1} + c_1 \theta + c_2 \phi + c_3 \Phi \theta + c_4 \Phi \phi + d_{1k} \exp(-g/p_1) + d_{2k} \exp(-g/p_2) + d_{3k} \cos((g - p_3)/p_4), \quad (10)$$

where A_k is the disk-equivalent reflectance (dimensionless), g is the absolute phase function (in degrees), θ and ϕ are the selenographic latitude and longitude, respectively, of the observer (in degrees), and Φ is the selenographic longitude of the Sun (degrees). As the illuminated fraction of the Moon is a function of the phase angle, disk-equivalent reflectances for ROLO measurements of a partially illuminated Moon are incorporated into the phase-dependent terms. In Eq. (10) the first polynomial represents the basic photometric function dependence on phase angle, disregarding any opposition effect. The second polynomial approximates the dependence on the face of the Moon that is illuminated, primarily representing the distribution of mare and highlands. The four terms with coefficients c_n represent the face of the Moon that is seen, with the way in which that face is illuminated taken into consideration. The form of the last three terms, each nonlinear in g , is strictly empirical: the first two represent the opposition effect, and the last one addresses a correlation found in the residuals after the fitting of the other variables. The surface of the Moon exhibits a strong increase in brightness at small phase angles, generally less than 4° . This retroreflection has historically been called the opposition effect.¹⁶

4. Comparison

A. SeaWiFS Input to the Comparison

The comparison between the SeaWiFS input and the USGS lunar model is made in terms of the lunar irradiance measured by the satellite instrument. For SeaWiFS this is the summed radiance from Eq. (1) multiplied by the solid angle for the SeaWiFS measurements, 2.56×10^{-6} sr³. For this comparison the SeaWiFS lunar measurements have been corrected for instrument change by use of the fitted curves in Fig. 9 [Eq. (6) and Table 1]. The corrections are the inverses of the fitted curves. And, as SeaWiFS oversamples the Moon in the along-track direction, the comparison requires the oversampling correction for the measurement from Eq. (4), which is provided as the along-track image size (mrad). In addition, the comparison requires that the times and

locations of the satellite during the measurements be known to allow the Sun–Moon and Moon–instrument distances, the phase angles, and the selenographic latitudes and longitudes to be calculated. Finally, the comparison requires knowledge of the spectral responses of the SeaWiFS bands.²⁵

For SeaWiFS the summed radiance, the solid angle of the measurements, and the oversampling correction are used to calculate the SeaWiFS-measured lunar irradiance, that is, the SeaWiFS version of Eq. (7) for the SeaWiFS bands. In a separate process the USGS lunar reflectance model is the basis for a parallel calculation of the same lunar irradiance, again for the SeaWiFS bands. It is these lunar irradiances that are compared below.

B. USGS Input to the Comparison

The time and location of the SeaWiFS lunar measurements provide the angles required for the solution of Eq. (10) for the disk-equivalent reflectances at the wavelengths of the ROLO telescope bands. However, the ROLO reflectances must be converted to those for the SeaWiFS bands. Seven of the eight SeaWiFS bands have wavelengths close to the corresponding ROLO bands (Table 4). Because the Moon's spectral features are broad and shallow, the conversion uses an interpolation between the ROLO wavelengths, with an additional factor that preserves the shape of the Apollo reference spectrum. The effective wavelength for the interpolation is calculated by use of this derived reflectance spectrum plus band averaging:

$$\lambda_{\text{eff}} = \frac{\int_{\lambda_1}^{\lambda_2} \lambda A_\lambda E_\lambda R_\lambda d\lambda}{\int_{\lambda_1}^{\lambda_2} A_\lambda E_\lambda R_\lambda d\lambda}, \quad (11)$$

where λ is the wavelength (nm), λ_{eff} is the effective wavelength for the SeaWiFS lunar measurement (nm), A_λ is the effective lunar disk reflectance at wavelength λ from the derived reflectance spectrum described above, E_λ is the solar irradiance at wavelength λ from the solar model of Wehrli,²⁶ and R_λ is the spectral response of the SeaWiFS band at wavelength λ . Because the lunar reflectance, the solar irradiance, and the SeaWiFS spectral response all appear in the numerator and the denominator of Eq. (11), their units cancel out of the result. The limits of integration give the wavelength range for the SeaWiFS spectral responses, which is 380–1150 nm.²⁵ The effective wavelength (λ_{eff}) is that of the radiance for a SeaWiFS lunar measurement, because the radiance is the product of the lunar reflectance and the solar irradiance. The calculation of the values of λ_{eff} for the SeaWiFS bands is made once, off line, by use of a nominal lunar reflectance curve. As the spectral shape of the lunar reflectance is virtually constant in the model, the values of λ_{eff} can be used as constants in a lookup table.

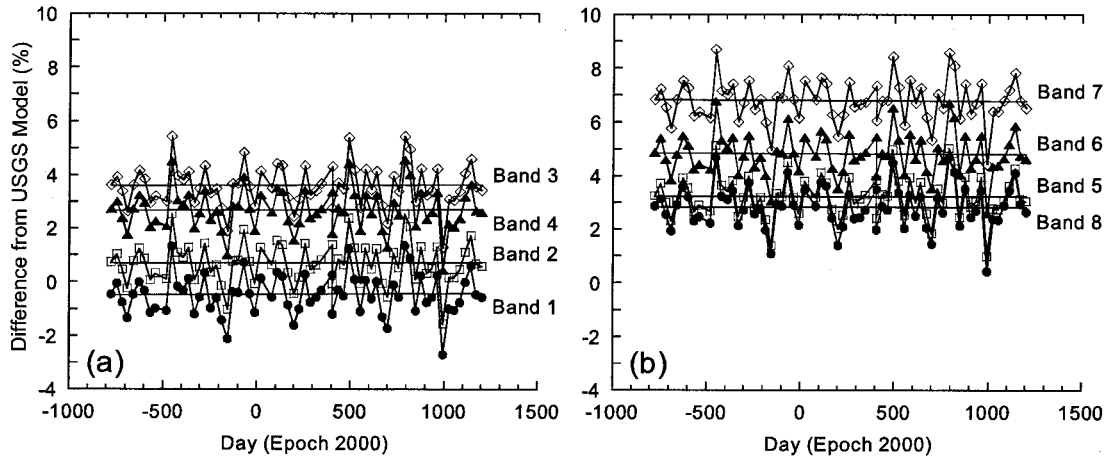


Fig. 12. Differences of the SeaWiFS lunar irradiances from the USGS model. The differences are in percent.

Because the Moon's spectral features are broad and shallow, the lunar reflectance at the SeaWiFS effective wavelength, $A_{\lambda_{\text{eff}}}$, is considered to be the lunar reflectance for the band, A_n , where n is the index for the SeaWiFS band (1–8). The lunar irradiance is calculated from this reflectance by

$$I_n = \frac{A_n \Omega_M E_n}{\pi}, \quad (12)$$

where I_n is the lunar irradiance for SeaWiFS band n ($\mu\text{W m}^{-2} \text{nm}^{-1}$), Ω_M is the solid angle of the Moon (sr^{-1}), and E_n is the solar irradiance for band n from Wehrli²⁶ ($\mu\text{W m}^{-2} \text{nm}^{-1}$). Equation (12) is similar to Eq. (9a). However, the reflectance and irradiance in Eq. (12) are for band n of SeaWiFS rather than for band k of the ROLO telescope.

The solar irradiance in Eq. (12) is calculated by band averaging:

$$E_n = \frac{\int_{\lambda_1}^{\lambda_2} E_\lambda R_\lambda d\lambda}{\int_{\lambda_1}^{\lambda_2} R_\lambda d\lambda}. \quad (13)$$

This is the same manner in which the value of E_k is calculated for Eqs. (9a) and (9b). The spectral response curves for the ROLO telescope are different from those of SeaWiFS, as are the limits of integration for the equation. Thus the consistency of the model (going into the model from the ROLO irradiances and coming out of the model to the SeaWiFS irradiances) depends on the wavelength consistency of the Wehrli²⁶ solar irradiance values. For the seven SeaWiFS bands with wavelengths close to corresponding bands in the ROLO telescope (Table 4), the solar irradiances should have minimal effects. However, SeaWiFS band 4 (510 nm) lies more than 20 nm from the closest ROLO telescope band. For SeaWiFS band 4, the Wehrli²⁶ irradiances are consistent with the MODTRAN²⁷ solar model and that of

Thuillier *et al.*²⁸ at the 0.5% level.²⁹ For the adjacent SeaWiFS bands, 490 and 555 nm, the agreement of the three solar irradiance models is better than 1.5%.²⁹ As a result, we believe that the effects of the Wehrli²⁶ model on the results presented below are less than 1.5%. And, because the solar irradiances are used as constants, the effects on the differences over time are negligible.

The final step in the conversion of the USGS reflectance model to SeaWiFS-measured irradiances is the conversion from the standard Moon–Sun and Moon–instrument distances to those of the actual SeaWiFS measurements, which is the inverse of that in Eq. (8). To ensure dimensional consistency in the comparison, the units for the SeaWiFS-measured lunar irradiances ($\text{mW cm}^{-2} \mu\text{m}^{-1}$) are converted to those for the USGS lunar model ($\mu\text{W m}^{-2} \text{nm}^{-1}$).

C. Comparison Results

The results of the comparison are given as the difference (in percent) of the SeaWiFS-measured lunar irradiances from the model-calculated values. This is the standard form for comparisons with the USGS model. For the 66 SeaWiFS measurements in this comparison, the results are shown in Fig. 12. The figure also shows the results of linear regressions for each band, which are essentially flat lines. The intercept for each band is given as the difference of the first SeaWiFS measurement in the data set. The slope for each band has units of percent per thousand days. As explained in Subsection 4.A, for this comparison the SeaWiFS lunar measurements have been corrected for instrument change by use of the fitted curves in Fig. 9 [Eq. (6) and Table 1]. The comparison is made after the application of those corrections.

Table 5 lists the slopes and intercepts for the linear regressions in Fig. 12. In addition, the table lists the standard deviation of the data points from the linear regression for each band. The slopes in Table 5 are small. Over the 2000 days of measurements, the total change for SeaWiFS band 1 relative to the USGS model is less than 0.1%. For band 7 the total

Table 5. Slopes and Intercepts for the Linear Regressions in Fig. 12^a

SeaWiFS Band	Wavelength (nm)	Intercept (%)	Slope (%/Thousand Days)	Standard Deviation (%)
1	413.0	-0.51	0.0484	0.76
2	444.1	0.69	0.0149	0.76
3	490.1	3.58	0.0122	0.78
4	510.3	2.66	0.0113	0.77
5	554.2	3.23	0.0022	0.78
6	668.8	4.82	-0.0104	0.79
7	763.8	6.82	-0.0178	0.79
8	866.4	2.84	-0.0016	0.80

^aThe data are the differences of the SeaWiFS lunar measurements from the USGS lunar model. The intercepts are the values of the fitted lines at the time of the first lunar measurement. The standard deviations (about the linear regressions) give a measure of the scatter in the data.

change is less than 0.04%, which is greater than the change for the remaining six bands. However, without the SeaWiFS instrument change corrections the differences from the USGS model would show shapes similar to those in Fig. 9. With the correction there is no significant trend in the calibration of SeaWiFS relative to the USGS lunar model. For the SeaWiFS calibration team these results are considered to be a test of the team’s lunar corrections.

The absolute differences in Fig. 12 derive from the calibrations of the two instruments. The calibration of SeaWiFS is based on prelaunch laboratory measurements of an integrating sphere.³⁰ The calibration of the ROLO telescope is based on measurements of the star Vega and on published values for that star in the astronomical literature.⁶ The estimated uncertainty for the SeaWiFS radiance measurements on orbit is 4–5%.⁸ This range approximates the sizes of the differences between instruments in Fig. 12 and Table 5.

There is a significant scatter in the data about the fitted curves in Fig. 12, with standard deviations of approximately 0.8%. The pattern in this scatter is nearly the same for each band. As a result, we attribute this scatter to the measurement-to-measurement uncertainty in the oversampling

correction for the along-track measurements, that is, to the oversampling error. Thus it is possible to apply the oversampling scattering correction, as discussed in Section 2 and shown in Fig. 8, to the results of the comparison. When this is done, the results are as shown in Fig. 13 and listed in Table 6. There are small differences in the intercepts and the slopes compared with those in Table 5. However, the standard deviations about the linear regressions are reduced by factors of 4–5 compared with those in Table 5. This is an indication that the large majority of the scatter in the comparison comes from the SeaWiFS measurements and not from some unknown lunar variation. The agreement between the slopes in Tables 5 and 6 is an indication that the oversampling correction does not change the calculated trends for the SeaWiFS lunar time series. As described in Subsection 2.D, the correction is designed to reveal the shapes of the trends in the bands with nonlinear lunar-based changes over time. Other than reducing the calculated standard deviations about the trend lines, the oversampling correction has no significant effect on the comparison.

There is a small common pattern to the scatter in Fig. 13, with intervals of approximately 0.5–1 year. This is different from the pattern of the scatter in Fig.

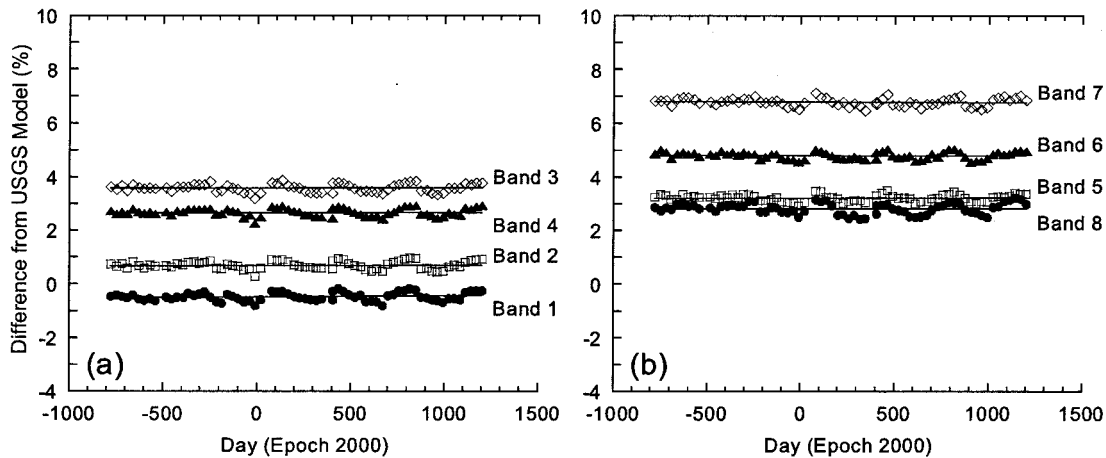


Fig. 13. Differences of the SeaWiFS lunar irradiances from the USGS model after correction for the oversampling scatter in the SeaWiFS measurements. The differences are in percent.

Table 6. Slopes and Intercepts for the Linear Regressions in Fig. 13^a

SeaWiFS Band	Wavelength (nm)	Intercept (%)	Slope (%/Thousand Days)	Standard Deviation (%)
1	413.0	-0.53	0.0476	0.15
2	444.1	0.67	0.0141	0.15
3	490.1	3.55	0.0113	0.15
4	510.3	2.64	0.0104	0.15
5	554.2	3.21	0.0014	0.13
6	668.8	4.80	-0.0110	0.13
7	763.8	6.79	-0.0184	0.15
8	866.4	2.82	-0.0025	0.20

^aThe data are the differences of the SeaWiFS lunar measurements from the USGS lunar model after correction for the oversampling scatter in the SeaWiFS measurements. The intercepts are the values of the fitted lines at the time of the first lunar measurement. The standard deviations (about the linear regressions) give a measure of the scatter in the data.

12, which is assumed to be dominated by the oversampling. The pattern in Fig. 13 has a standard deviation that is approximately twice that for the fitted curves in Fig. 9 (Table 2). As a result, we have concluded that half, or more, of the scatter in Fig. 13 comes from the comparison with the USGS model and that the remaining scatter is caused by imperfect correction for the oversampling error. Also, the results in Fig. 13 show the level of agreement that can be reached in comparisons of Earth imaging instruments with the USGS model, particularly in terms of changes in the radiometric calibrations of the instruments over time.

5. Concluding Remarks

The SeaWiFS measurements of the Moon are independent from those of the ROLO telescope. However, the claim of independence of the two techniques must be tempered by knowledge of the similarities in the methods of analysis. Both sets of measurements apply corrections for distances and phase angles and for changes in the portion of the Moon that is observed over time. If this set of corrections is appropriate, then the agreement in the instrument response histories for the two techniques provides a validation of the USGS lunar model by SeaWiFS over the range of SeaWiFS phase angles and vice versa.

As the SeaWiFS mission continues, the understanding of the measurements also continues to develop. As of this writing in 2004, the SeaWiFS project has completed its fourth update of the data set with a reprocessing in July 2002.³¹ A fifth reprocessing of the data set, in 2005, is anticipated. Before the July 2002 reprocessing, long-term instrument changes in the data set were based on the assumption that, on average, the 490- and 510-nm bands were not changing over time.^{8,14} We calculated the changes in the other instrument bands by normalizing the output of each band to the average of the 490- and 510-nm bands.^{8,14} In early 2002 a comparison was made with a preliminary version of the USGS lunar model. Based on that comparison, an average change rate of 0.35% per thousand days for those two bands was incorporated into the fourth reprocessing as a substitute for the earlier

assumption.³¹ Changes for the individual bands were determined by the same normalization to the 490- and 510-nm bands. At that time, the inability of the SeaWiFS calibration team to correct the libration-based oscillations in the lunar data set precluded an independent determination of instrument changes. With the developed understanding of libration presented here it is now possible to determine the changes in each SeaWiFS band without the need for the USGS lunar model as a reference. Also, the instrument changes presented here are nearly identical to those from the fourth reprocessing. The average of the linear change rates for the 490- and 510-nm bands in Table 1 is 0.32% per thousand days.

A developed understanding of libration and other factors in a lunar time series comes from the analysis of an extended data set. The results presented here are based on 66 lunar measurements by SeaWiFS. For satellite instruments at the beginning of on-orbit operations, when the number of lunar measurements is limited, the USGS model is critical to an understanding of instrument trends that use the Moon for calibration.

For ocean color measurements the determination of instrument changes at the level presented here is important. The ocean is dark, and most of the top-of-the-atmosphere radiance over oceans comes from the atmosphere. Thus the calculation of the radiance leaving the ocean surface from top-of-the-atmosphere measurements comes from the small difference between two large numbers. Small changes in the calibration of the satellite instrument can cause large changes in the water-leaving radiances, with a multiplying factor of ~10. The deep ocean gyres, where the water is clear and the chlorophyll concentrations are small, provide sensitive locations for monitoring instrument changes. Over periods of several years or more, the conditions of the gyres are not expected to change, nor are the average water-leaving radiances.³² With the current lunar-based determination of the calibration history of SeaWiFS, the trends in the global mean clear-water water-leaving radiances measured by SeaWiFS are less than 0.5% per thousand days.³¹ The assumption of no long-term geophysical change in the deep

oceans is central to the interpretation of this result. For satellite calibration purposes, however, the lunar surface is photometrically stable over the period of 10^8 years.⁴

The libration corrections presented here are not part of the latest processing of SeaWiFS (Reprocessing 4, July 2002). Other changes from Reprocessing 4 include calculation of the illuminated fraction of the Moon and of the along-track size of the Moon in Eq. (4). It is anticipated that these changes will be incorporated into the next SeaWiFS reprocessing. Also, the fitted forms for the time-dependent changes in SeaWiFS bands 3–5, 7, and 8 in Eq. (6) differ from the form for instrument change in Reprocessing 4, in which each band was treated as a single exponential.³¹

At the time of the fifth SeaWiFS reprocessing there will be an expanded set of lunar measurements available for analysis. In addition, it may be possible to incorporate the efficiencies of the USGS computational technique given in Eq. (10) into the SeaWiFS libration correction. The form of Eq. (10) that uses the lunar irradiance in logarithmic space provides a potentially improved method for calculating the SeaWiFS libration coefficients compared with the current multiplicative technique. However, these changes should not affect the overall agreement of the SeaWiFS measurements with the USGS lunar model.

Support for this research was provided in part by NASA contact NAS5-00141 and by interagency agreement S-41359-F.

References

- W. A. Hovis, D. K. Clark, F. Anderson, R. W. Austin, W. H. Wilson, E. T. Baker, D. Ball, H. R. Gordon, J. L. Mueller, S. Z. El-Sayed, B. Sturm, R. C. Wrigley, and C. S. Yentsch, "Nimbus-7 Coastal Zone Color Scanner: system description and initial imagery," *Science* **210**, 60–62 (1980).
- C. R. McClain, W. E. Esaias, W. Barnes, B. Guenther, D. Endres, S. B. Hooker, B. G. Mitchell, and R. Barnes, *SeaWiFS Calibration and Validation Plan*, NASA Tech. Memo. 104566, Vol. 3, S. B. Hooker, and E. R. Firestone, eds. (NASA Goddard Space Flight Center, Greenbelt, Md., 1992).
- R. A. Barnes, W. L. Barnes, W. E. Esaias, and C. R. McClain, *Prelaunch Acceptance Report for the SeaWiFS Radiometer*, NASA Tech. Memo. 104566, Vol. 22, S. B. Hooker, E. R. Firestone, and J. G. Acker, eds. (NASA Goddard Space Flight Center, Greenbelt, Md., 1994).
- H. H. Kieffer, "Photometric stability of the lunar surface," *Icarus* **130**, 323–327 (1997).
- H. H. Kieffer, T. C. Stone, R. A. Barnes, S. Bender, R. E. Eplee, Jr., J. Mendenhall, and L. Ong, "On-orbit radiometric calibration over time and between spacecraft using the Moon," in *Sensors, Systems, and Next-Generation Satellites VI*, H. Fujisada, J. B. Lurie, M. L. Aten, and K. Weber, eds., Proc. SPIE **4881**, 287–298 (2003).
- T. C. Stone and H. H. Kieffer, "Absolute irradiance of the Moon for on-orbit calibration," in *Earth Observing Systems VII*, W. L. Barnes, ed., Proc. SPIE **4814**, 211–221 (2002).
- R. A. Barnes, A. W. Holmes, W. L. Barnes, W. E. Esaias, C. R. McClain, and T. Svitek, *SeaWiFS Prelaunch Radiometric Calibration and Spectral Characterization*, NASA Tech. Memo. 104566, Vol. 23, S. B. Hooker, E. R. Firestone, and J. G. Acker, eds. (NASA Goddard Space Flight Center, Greenbelt, Md., 1994).
- R. A. Barnes, R. E. Eplee, Jr., G. M. Schmidt, F. S. Patt, and C. R. McClain, "Calibration of SeaWiFS. I. Direct techniques," *Appl. Opt.* **40**, 6682–6700 (2001).
- R. A. Barnes, R. E. Eplee, Jr., and F. S. Patt, "SeaWiFS measurements of the Moon," in *Sensors, Systems, and Next Generation Satellites II*, H. Fujisada, ed., Proc. SPIE **3498**, 311–324 (1998).
- R. A. Barnes, R. E. Eplee, Jr., F. S. Patt, and C. R. McClain, "Changes in the radiometric sensitivity of SeaWiFS determined from lunar and solar-based measurements," *Appl. Opt.* **38**, 4649–4664 (1999).
- P. Helfenstein and J. Veverka, "Photometric properties of lunar terrains derived from Hapke's equations," *Icarus* **72**, 342–357 (1987).
- A. P. Lane and W. M. Irvine, "Monochromatic phase curves and albedos for the lunar disk," *Astron. J.* **78**, 267–277 (1973).
- R. A. Barnes and C. R. McClain, "The calibration of SeaWiFS after two years on orbit," in *Sensors, Systems, and Next-Generation Satellites III*, H. Fujisada, ed., Proc. SPIE **3870**, 214–227 (1999).
- C. R. McClain, E. J. Ainsworth, R. A. Barnes, R. E. Eplee, Jr., F. S. Patt, W. D. Robinson, M. Wang, and S. W. Bailey, *SeaWiFS Postlaunch Calibration and Validation Analyses, Part 1*, NASA Tech. Memo. 2000-206892, Vol. 9, S. B. Hooker and E. R. Firestone, eds. (NASA Goddard Space Flight Center, Greenbelt, Md., 2000).
- R. E. Eplee, Jr., R. A. Barnes, F. S. Patt, G. Meister, and C. R. McClain, "SeaWiFS lunar calibration methodology after six years on orbit," in *Earth Observing Systems IX*, W. L. Barnes and J. J. Butler, eds., Proc. SPIE **5542** (to be published).
- B. J. Buratti, J. K. Hillier, and M. Wang, "The lunar opposition surge: observations by Clementine," *Icarus* **124**, 490–499 (1996).
- R. H. Evans and H. R. Gordon, "Coastal Zone Color Scanner 'system calibration': a retrospective examination," *J. Geophys. Res.* **99**, 7293–7307 (1994).
- R. A. Barnes and E. F. Zalewski, "Reflectance-based calibration of SeaWiFS. I. Calibration coefficients," *Appl. Opt.* **42**, 1629–1647 (2003).
- R. A. Barnes, R. E. Eplee, Jr., S. F. Biggar, K. J. Thome, P. N. Slater, and A. W. Holmes, "SeaWiFS transfer-to-orbit experiment," *Appl. Opt.* **39**, 5620–5631 (2000).
- H. H. Kieffer and J. M. Anderson, "Use of the Moon for spacecraft calibration over 350–2500 nm," in *Sensors, Systems, and Next Generation Satellites II*, H. Fujisada, ed., Proc. SPIE **3498**, 325–336 (1998).
- J. M. Anderson, K. J. Becker, H. H. Kieffer, and D. N. Dodd, "Real-time control of the Robotic Lunar Observatory," *Publ. Astron. Soc. Pac.* **111**, 737–749 (1999).
- T. C. Stone, H. H. Kieffer, and K. J. Becker, "Modeling the radiance of the Moon for on-orbit calibration," in *Earth Observing Systems VIII*, W. L. Barnes, ed., Proc. SPIE **5151**, 463–470 (2003).
- F. E. Nicodemus, J. C. Richmond, J. J. Hsia, I. W. Ginsberg, and T. Limperis, *Geometrical Considerations and Nomenclature for Reflectance*, NBS Monogr. 160 (National Bureau of Standards, Washington, D.C., 1977).
- P. Y. Barnes, E. A. Early, and A. C. Paar, *Spectral Reflectance*, NIST Spec. Publ. SP 250-48 (National Institute of Standards and Technology, Gaithersburg, Md., 1998).
- R. A. Barnes, "SeaWiFS data: actual and simulated" (NASA Goddard Space Flight Center, Greenbelt, Md., 1994), available from <http://seawifs.gsfc.nasa.gov/SEAWIFS/IMAGES/spectra1.dat> and [/spectra2.dat](http://seawifs.gsfc.nasa.gov/SEAWIFS/IMAGES/spectra2.dat).
- C. Wehri, "Spectral solar irradiance data," World Climate

- Research Program (WCRP) Publ. Ser. 7, WMO ITD 149 (World Meteorological Organization, Geneva, Switzerland, 1986), pp. 119–126.
27. A. Berk, L. S. Bernstein, and D. C. Robertson, "MODTRAN: a moderate resolution model for LOWTRAN7," Tech. Rep. GL-TR-90-0122 (Phillips Laboratory, Hanscom Air Force Base, Mass., 1989).
 28. G. Thuillier, M. Hersé, P. C. Simon, D. Labs, H. Mandel, D. Gillotay, and T. Foujols, "The solar spectral irradiance from 200 to 2400 nm as measured by the SOLSPEC spectrometer from the ATLAS 1-2-3 and EURECA missions," *Sol. Phys.* **214**, 1–22 (2003).
 29. R. A. Barnes and E. F. Zalewski, "Reflectance-based calibration of SeaWiFS. II. Conversion to radiance," *Appl. Opt.* **42**, 1648–1660 (2003).
 30. B. C. Johnson, E. A. Early, R. E. Eplee, Jr., R. A. Barnes, and R. T. Caffrey, *The 1997 Prelaunch Calibration of SeaWiFS*, NASA Tech. Memo. 1999-206892, Vol. 4, S. B. Hooker and E. R. Firestone, eds. (NASA Goddard Space Flight Center, Greenbelt, Md., 1999).
 31. F. S. Patt, R. A. Barnes, R. E. Eplee, Jr., B. A. Franz, W. D. Robinson, G. C. Feldman, S. W. Bailey, J. Gales, P. J. Werdell, M. Wang, R. Frouin, R. P. Stumpf, R. A. Arnone, R. W. Gould, Jr., P. M. Martinolich, V. Ransibrahmanakul, J. E. O'Reilly, and J. A. Yoder, in *Algorithm Updates for the Fourth SeaWiFS Data Reprocessing*, NASA Tech. Memo. 2003-206892, Vol. 22, S. B. Hooker and E. R. Firestone, eds. (Goddard Space Flight Center, Greenbelt, Md., 2003).
 32. R. E. Eplee, Jr., W. D. Robinson, S. W. Bailey, D. K. Clark, P. J. Werdell, M. Wang, R. A. Barnes, and C. R. McClain, "Calibration of SeaWiFS. II. Vicarious techniques," *Appl. Opt.* **40**, 6701–6718 (2001).